Observation of thermal transport close to diffusive in a weak long-ranged Fermi-Pasta-Ulam-Tsingou-type model

Daxing Xiong [1,*] and Jianjin Wang [2,†]

[1]*MinJiang Collaborative Center for Theoretical Physics, College of Physics and Electronic Information Engineering,*
Minjiang University, Fuzhou 350108, China
[2]*Department of Physics, Jiangxi Science and Technology Normal University, Nanchang 330013, Jiangxi, China*

We explore thermal transport in a one-dimensional Fermi-Pasta-Ulam-Tsingou-type (FPUT-type) system with long-range (LR) interactions. In such a system, the harmonic part of the potential is nearest-neighbor coupled, while the strength of the quartic part of the potential between two lattice sites decays as a power σ of the inverse of their distance, demonstrating the LR feature of the system. The relevant strong LR model ($0 \leqslant \sigma \leqslant 1$) has been considered in detail in our recent study [Xiong and Wang, Phys. Rev. E **109**, 044122 (2024)], and here, we focus on the weak LR regime ($1 \leqslant \sigma \leqslant 3$). We show that the thermal transport behaviors in this regime are quite unexpected. We discovered a subregime ($1 \leqslant \sigma \leqslant 1.5$) wherein the thermal transport behaviors are very close to diffusive. This suggests that even a momentum-conserving system with appropriate LR interactions can still exhibit normal heat conduction. By meticulously analyzing the space-time scaling properties of equilibrium heat correlations, we also determine the center of this diffusive thermal transport at approximately $\sigma \simeq 1.25$. These discoveries, together with our prior results, provide a comprehensive understanding of thermal transport of this kind of LR-FPUT-type model.

I. INTRODUCTION

In recent years, research has intensified on long-range (LR) interactions, spanning from cosmic scales [1] to nanoscale intricacies [2]. These systems are defined by interaction potentials $V(r)$ that decay as a power law:

$$V(r) \propto \frac{1}{r^{\sigma}}, \qquad (1)$$

where r is the distance between particles. These interactions give rise to systems with intricate dynamics and thermal properties, distinct from those with short-range (SR) interactions. They often display unique phenomena such as nonergodicity, weak chaos, ensemble inequivalence, long-lived non-Gaussian states, one-dimensional (1D) phase transitions, nonconcave entropy, and even negative specific heat (see reviews [3–6]). These exceptional features challenge the classical Boltzmann-Gibbs statistical mechanics framework. The complexity of LR interacting systems makes them an intriguing yet demanding field of study.

Despite widespread anticipation that interaction range would significantly influence thermal transport, our main understandings have honed in on systems with nearest-neighbor

(NN) couplings [7–9]. It is only in more recent times that the thermal transport properties of systems with LR interactions have begun to attract the interest of the community [10–12]. Within this burgeoning field, several paradigmatic models have been introduced and studied, including the LR variants of rotor, Fermi-Pasta-Ulam-Tsingou (FPUT), lattice ϕ^4, and harmonic models. Specific attention has been devoted to the σ-dependent thermal transport within both nonlinear rotor and FPUT-type models, both with features of conserved momentum [13–26]. The LR-rotor model demonstrated a transition between two phases: an insulating phase when the interaction strength is strong (for $0 < \sigma < 1$) and a conductive phase for $\sigma > 1$ [13]. Intriguingly, in the strong LR regime, a flat temperature profile is exhibited, reminiscent of the behavior in integrable systems [13], implying its connection to integrability. However, subsequent analysis [16] indicated that this phenomenon is driven by an alternative mechanism of parallel energy transport rather than the integrability. Moreover, the subdiffusive energy transport mechanism witnessed in the insulator phase under the mean-field case ($\sigma = 0$) was validated numerically in Ref. [15].

In the exploration of LR-FPUT models, the LR interactions can be added through two distinct forms including the LR-quartic term only [14,18,20,21] or melding both quadratic and quartic LR terms [16,17]. Viewing this difference, in the following, we denote the former as the *LR-quartic* model and the latter as the *LR-quadratic-quartic* model. With both kinds of models, more complex and intriguing transport phenomena than those observed in the LR-rotor model have been unveiled. A particularly noteworthy finding [14] is the behavior exhibited at a specific interaction range value of $\sigma = 2$, where the

*Contact author: xmuxdx@163.com
†Contact author: phywjj@foxmail.com

thermal conductivity κ of the system exhibits a near-linear divergence with the system size N, accompanied by an almost flat temperature profile. Note that, for 1D anharmonic momentum-conserving lattices with SR NN interactions only, it has been believed that κ diverges with N in a power law:

$$\kappa \sim N^{\alpha}, \tag{2}$$

with $0 < \alpha \leqslant 1$ the divergence exponent. Therefore, a linear dependence of κ vs N means $\alpha = 1$. This ballistic-like transport suggests the existence of an as-yet undiscovered integrable limit of the model at $\sigma = 2$ [11,12]. However, it is important to note that the LR-FPUT system under consideration is inherently nonintegrable. Authors of a subsequent investigation [18] meticulously examined the impacts of reservoir and boundary conditions on the transport of the system and revealed a superdiffusive transport with a notably high divergent exponent $\alpha \simeq 0.7$, which is substantially greater than $\alpha \simeq 0.3$–0.5 typically observed in SR interacting systems with NN couplings. This special superdiffusive transport at $\sigma = 2$ was further characterized by a slower decay in energy current correlations and was linked to a weaker nonintegrability mechanism and the emergence of a unique class of traveling discrete breathers (DBs) within the system, which serve to enhance thermal transport [18]. While the validity of this superdiffusive thermal transport was later questioned in Ref. [20], the collective body of work [14,16,18,20] affirms the unique features observed at $\sigma = 2$, irrelevant to the models of LR-quadratic-quartic or LR-quartic type.

Beyond the intriguing behaviors observed at $\sigma = 2$, the thermal transport generally exhibits distinct properties across different σ regimes [10]. Specifically, three typical regimes can be identified: (i) strong LR regime ($0 \leqslant \sigma \leqslant 1$), (ii) weak LR regime ($1 < \sigma \leqslant 3$), and (iii) SR regime ($\sigma > 3$). For the SR regime, two existing works for the LR-quartic model [14] and the LR-quadratic-quartic model [16] have consistently indicated anomalous superdiffusive transport, with the transport exponent α ranging from 0.3 to 0.5. Authors of a notable analysis [19], based on a linear LR-harmonic system involving stochastic momentum exchange dynamics, corroborated this trend, suggesting a value of $\alpha = 0.5$.

For both strong and weak LR regimes, usually a prefactor $\frac{1}{\widehat{N}}$, denoted as

$$\widehat{N} = \frac{1}{N} \sum_{i} \sum_{i \neq j} \frac{1}{|i - j|^{\sigma}}, \tag{3}$$

with $|i - j|$ being the (shortest) distance between the lattice sites i and j, i.e., the Kac scaling factor, is employed and added to the corresponding LR interactions to make the Hamiltonian of the system extensive. Now if one turns to the current achievements of thermal transport: For the strong LR regime, the early numerical study for the LR-quartic model with $\frac{1}{\widehat{N}}$ included [14] suggested anomalous superdiffusive transport as well but with an exponent $\alpha > 0.5$. Authors of a subsequent study of the LR-quadratic-quartic model (including $\frac{1}{\widehat{N}}$ as well) [16] suggested the same parallel energy transport mechanism as the LR-rotor model, and based on this mechanism, ballistic thermal transport in the strong LR regime would be expected [10]. On the other hand, the analytical findings [19] were unable to provide

conclusive results for this regime. Another result of ours focusing on a LR-quartic model without including $\frac{1}{\widehat{N}}$ however gave a significantly different scenario [21,22]. We have revealed subdiffusive transport behaviors both in the mean-field and beyond the mean-field cases of the model, akin to that observed in the mean-field case of the LR-rotor system [15]. Remarkably, we have also found another special point of $\sigma = 0.5$ characterizing two distinct subdiffusive behaviors based on the antipersist energy current correlations of the system [22].

Lastly, in the weak LR regime, both the existing numerical studies of the LR-quartic [14] and the LR-quadratic-quartic [16] models, both with $\frac{1}{\widehat{N}}$ included, consistently indicated anomalous superdiffusive transport. When $1 \leqslant \sigma < 2$, Ref. [14] suggested that the exponent α hovers $\sim$0.3, while Ref. [16] indicated $\alpha \sim 0.6$. For $2 < \sigma \leqslant 3$, both gave the value of α decreasing from $\alpha = 1$ to a value range from $\sim$0.4 to 0.5. The analytical results [19] could not predict the behavior $1 \leqslant \sigma < 2$ but did offer insights for $2 < \sigma \leqslant 3$, indicating that α would decrease from $\alpha = 1$ and stabilize at $\alpha = 0.5$ once σ exceeds 3.

It is also worth noting that recent relevant progress also includes studies in the momentum-nonconserving LR-ϕ^4 model [23], the momentum-conserving LR-harmonic systems in the mean-field limit [24,25], and LR-harmonic model within the strong LR regime beyond the mean-field case [26].

In view of the above background, a comprehensive understanding of thermal transport in the LR-FPUT type models, particularly for the weak LR regime, is still lacking. On one hand, the analytical results [19] failed to predict the behavior for $1 \leqslant \sigma < 2$, leaving a theoretical gap in our understanding. On the other hand, current numerical results in this regime for different models predict different values of α, which are somewhat a little confused [14,16]. In this respect, it is also important to note that distinct simulation methods to derive thermal conductivity κ were employed; Ref. [14] utilized thermostats added to harmonic leads, whereas Ref. [16] employed Maxwellian heat baths, which does not need additional harmonic leads. Furthermore, employing the LR-quartic and LR-quadratic-quartic models with or without including the Kac scaling factor seems to cause significant disparity regarding thermal transport in the strong LR regime. Two early results yielded superdiffusive [14] and ballistic [16] transport behaviors, for the LR-quartic and LR-quadratic-quartic models, respectively, both including $\frac{1}{\widehat{N}}$. In contrast, based on the energy current correlation and the spatiotemporal correlation function of heat, our quite recent results [21,22] for the LR-quartic model without including $\frac{1}{\widehat{N}}$ provided compelling evidence supporting subdiffusive behavior. Given the significant role that LR interactions also play in the weak LR regime, this paper is devoted to investigating in detail the thermal transport of the LR-quartic model (without including $\frac{1}{\widehat{N}}$) within this weak LR regime, as the studies of the same model within the strong LR regime have already revealed quite rich transport and microscopic dynamics [21,22].

The remainder of this paper is structured as follows: In Sec. II, we outline the specific LR-quartic model under examination within the weak LR regime, along with the specifics of the numerical techniques employed. Section III presents our findings on the σ-dependent energy current correlation

within this regime, from which possible signatures of thermal transport close to diffusive within the interval $1 \leqslant \sigma \leqslant 1.5$ are given. Section IV is devoted to the results of σ-dependent equilibrium heat correlations, with our particular focus on its scaling behaviors. Here, the behaviors of thermal transport close to diffusive have been confirmed with high precision. Section V demonstrates the thermal transport phase diagram for all $\sigma > 0$. Finally, we summarize our findings succinctly in Sec. IV, followed by a discussion.

II. MODEL AND METHOD

We examine a 1D FPUT-type LR interacting system composed of N particles with Born–von Kármán periodic boundary conditions [27], where the dynamics is dictated by the Hamiltonian:

$$H = \sum_{i=1}^{N} \left[\frac{p_i^2}{2} + \frac{1}{2}(x_{i+1} - x_i)^2 + \frac{1}{4} \sum_{r=1}^{(N/2)-1} \frac{(x_{i+r} - x_i)^4}{r^\sigma} \right]. \tag{4}$$

In this Hamiltonian, x_i and p_i represent two canonically conjugated variables, with i denoting the particle index; all other relevant quantities, such as the mass of the particle and the lattice constant, are dimensionless and set to unity. The periodic boundary conditions employed render our system akin to a ring, which are used to facilitate our following equilibrium simulations. The interparticle interaction comprises two distinct components, consistent with our previous works [18,21,22]. As mentioned in the Introduction, this is referred to as a LR-quartic model, i.e., the NN couplings are incorporated into the quadratic potential term, while the LR interactions are included in the quartic potential term. In the LR potential term, $r^{-\sigma}$ signifies the interaction strength between the ith particle and rth neighbor, with σ representing the LR exponent range value. This configuration of the LR-FPUT model, featuring solely the LR-quartic potential term, has been observed to exhibit more intriguing dynamic phenomena than models incorporating both LR-quadratic and quartic potential terms [28,29]. Hence, in this paper, we will focus exclusively on this configuration.

Following our previous works [18,21,22], we do not incorporate the Kac scaling factor $\frac{1}{N}$ into the LR potential term. By doing so, we are not here to say the factor $\frac{1}{N}$ is unimportant, while our choice is predicated on the following observations, i.e., while $\frac{1}{N}$ was intended to restore the extensivity of the system as the system size increases, it does not enhance the nonadditivity of the system [4]. Rather, it merely constructs an artificial extensive system yet at the expense of necessitating that both the group velocity of the phonon and the strength of nonlinearity depend on N, an undesirable outcome for thermal transport studies [18]. Furthermore, the dynamical time required to achieve equilibrium is extended by a factor of $\sqrt{N}$ when the Kac scaling factor is included [30]. Notably, a system characterized by the Hamiltonian in Eq. (4) at $\sigma = 2$ without including the Kac scaling factor has been demonstrated to possess a unique symmetric characteristic and supports a distinctive class of free-tail traveling DBs [18,31]. Such results serve as some justifications for excluding the Kac scaling factor from the model.

As previously outlined in the Introduction, in this investigation, we will focus on the thermal transport in the weak LR regime. Since in a previous work [22] we have found that the antipersistent energy current correlations for demonstrating subdiffusive transport eventually vanish for $\sigma > 0.7$, here, we will consider the regime beginning with $\sigma = 0.8$, i.e., $0.8 \leqslant \sigma \leqslant 3$. To capture the transport behavior of the system, we will examine the following two main physical quantities: (i) the equilibrium energy current time (t) autocorrelation of the system, expressed as

$$C_{JJ}(t) = \langle J_{\text{tot}}(t) J_{\text{tot}}(0) \rangle, \tag{5}$$

and (ii) the equilibrium spatiotemproal correlation function of the local thermal energy, defined by [18,32]

$$\rho_Q(m,t) = \frac{\langle \Delta Q_{l+m}(t) \Delta Q_l(0) \rangle}{\langle \Delta Q_l(0) \Delta Q_l(0) \rangle}. \tag{6}$$

In Eq. (5), J_{tot} is the total heat current along the system, defined by

$$J_{\text{tot}} = \sum_{i=1}^{N} p_i \left[(x_{i+1} - x_i) + \sum_{r=1}^{(N/2)-1} \frac{(x_{i+r} - x_i)^3}{r^\sigma} \right]. \tag{7}$$

It is noteworthy that this energy current includes both SR and LR contributions, differing from the definition provided in Ref. [14] by incorporating harmonic lead sites. Consequently, the computation of our definition presents challenges. For systems exhibiting diffusive and superdiffusive transport, $C_{JJ}(t)$ is linked to the thermal conductivity κ via the Green-Kubo relation [19]:

$$\kappa = \lim_{\tau \to \infty} \lim_{N \to \infty} \frac{1}{k_B N T^2} \int_0^\tau C_{JJ}(t) dt, \tag{8}$$

where k_B denotes the Boltzmann constant and T represents the system¡¯s equilibrium temperature. The diffusive thermal transport is usually related to an exponential time decay of $C_{JJ}(t)$ faster than t^{-1}, leading to a finite κ. However, in systems that may exhibit subdiffusive transport, the energy current correlation $C_{JJ}(t)$ is ill defined [19]. Such systems display an antipersistent correlation characterized by negative correlation values [21,22].

In Eq. (6), $\langle \cdot \rangle$ denotes the spatiotemporal average; l labels the number of particles in a coarse-grained bin (in practice, we set each bin of 8 particles); $Q_l(t) = E_l(t) - \frac{(\langle E \rangle + \langle F \rangle) g_l(t)}{\langle g \rangle}$ represents the local thermal energy, with $g_l(t)$ the particle number density, $E_l(t) = \sum_i E_i(t)$ the energy density within the lth bin [where $E_i = \frac{p_i^2}{2} + \frac{1}{2}(x_{i+1} - x_i)^2 + \frac{1}{4} \sum_{r=1}^{(N/2)-1} \frac{(x_{i+r} - x_i)^4}{r^\sigma}$], and $F_l(t)(\langle F \rangle \equiv 0)$ the pressure density, respectively. We note that, due to the translational invariance, $\rho_Q(m,t)$ solely depends on the relative distance m. Hence, if the values of $g_l(t)$, $E_l(t)$ in the ith bin, and $F_l(t)$ exerted on the ith bin at each time t are known, $\rho_Q(m,t)$ can be computed by an ensemble average.

To compute $C_{JJ}(t)$ and $\rho_Q(m,t)$ numerically, for each σ, we consider two total system sizes of $N = 4096$ and 8192 (some of the results for $\sigma > 1.5$ are under a larger system size). We generate a fully thermalized system at the equilibrium averaged temperature of $T = 0.5$, and during the computations, the system then is isolated. The system evolves
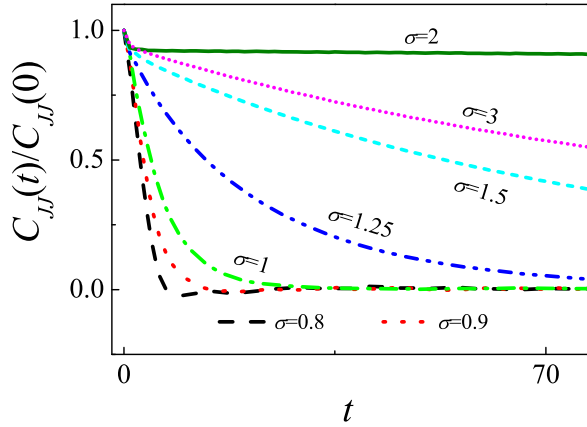
FIG. 1. $C_{JJ}(t)$ vs t for several σ within $0.8 \leqslant \sigma \leqslant 3$. Here, for a better visualization, the correlation values have been rescaled between 0 and 1 by dividing them with $C_{JJ}(0)$.

FIG. 2. The same as Fig. 1 but depicted in a log-log plot to identify the exponential and power-law decay behaviors.

using the velocity-Verlet algorithm [33] with a minute time step of 0.01, ensuring energy conservation with a relative accuracy of $O(10^{-5})$. To expedite our calculations, we employ a fast Fourier transform algorithm [34]. This approach circumvents the need for $O(N^2)$ operations in computing forces at each time step within our system. An ensemble of size $\sim 8 \times 10^9$ is utilized to determine the correlations.

III. ENERGY CURRENT CORRELATIONS

Now let us start with the results of energy current correlations. Figure 1 depicts $C_{JJ}(t)$ as a function of the time lag t across various LR exponents σ, ranging from $0.8 \leqslant \sigma \leqslant 3$, within a relatively short time frame of $t < 100$. The purpose of this plot is to clearly observe the absence of antipersistent behavior in $C_{JJ}(t)$, as previously indicated in Ref. [22], while fortunately, it also uncovers findings. As can be seen, for $\sigma = 0.8$, we successfully replicate the antipersistent correlation observed in Ref. [22], albeit with a small magnitude ($|C_{JJ}(t)|$) for the negative minimum value. As σ increases within the range of $0.8 \leqslant \sigma \leqslant 3$, an intriguing and nonmonotonic trend emerges, wherein a crossover from antipersistent correlation to fast exponential-like decay (centered around $\sigma \simeq 1.25$) appears for $0.8 \leqslant \sigma \leqslant 1.5$. Beyond $\sigma = 1.5$, initially, $C_{JJ}(t)$ exhibits an almost nonzero plateau with minimal decay at $\sigma = 2$. Subsequently, for values exceeding $\sigma > 2$ (e.g., see $\sigma = 3$), the decay rate of $C_{JJ}(t)$ becomes rapid but still remains lower than the exponential-like decay observed in $\sigma = 1.5$. This intriguing result not only further substantiates the uniqueness associated with $\sigma = 2$, consistent with previous observations [14,16,18] but also suggests possibilities regarding normal diffusive thermal transport within the regime of $1 \leqslant \sigma \leqslant 1.5$, based on its exponential-like decay behavior. To investigate the decay behavior of $C_{JJ}(t)$ over a long time and determine whether it follows an exponential or a power-law decay, it is customary to present the results of $C_{JJ}(t)$ vs t in a log-log plot, as shown in Fig. 2. The data presented here are identical to those in Fig. 1 but with longer time exhibited. As observed, for $\sigma = 2$, we reproduce the slow decay of $C_{JJ}(t) \sim t^{-0.15}$ (indicated by one of the lines with short dash-dot), which is consistent with our previous findings reported in Ref. [18],
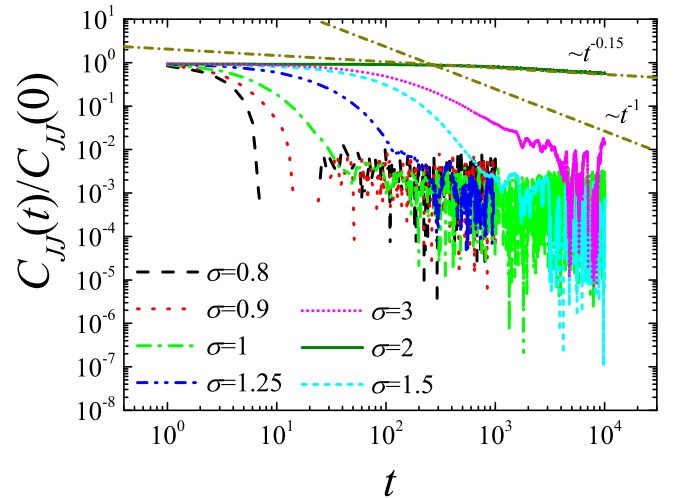
demonstrating superdiffusive transport at this σ value. Conversely, all values of $C_{JJ}(t)$ within $0.8 \leqslant \sigma \leqslant 1.5$ exhibit faster decay than that predicted by $C_{JJ}(t) \sim t^{-1}$, indicating convergence toward a finite thermal conductivity via Green-Kubo integral analysis described by Eq. (8). This observation corroborates our earlier conclusion based on Fig. 1 regarding diffusive thermal transport characteristics under these conditions. Regarding $\sigma = 3$, we note that, although our current data suggest faster decay rates for $C_{JJ}(t)$ than those predicted by $C_{JJ}(t) \sim t^{-1}$, this may be attributed to finite-sized effects on correlation functions during simulations [35] since $\sigma = 3$ is close to SR cases. At present, for all σ values considered, we are unable to provide more reliable data for evaluating the behavior of $C_{JJ}(t)$ in a longer time, as we are considering a LR interacting system.

IV. EQUILIBRIUM SPATIOTEMPROAL CORRELATION OF THERMAL ENERGY

Considering the challenges posed by $C_{JJ}(t)$ in investigating the long-term transport behavior here, we now present the results of equilibrium spatiotemporal correlation analysis for local thermal energy. Figure 3 illustrates $\rho_Q(m, t)$ at three different long times within the range $0.9 \leqslant \sigma \leqslant 3$. It is worth noting that, for $0.9 \leqslant \sigma \leqslant 1.5$, our analysis is based on a system size of $N = 4096$ and allows us to explore a long time up to $t = 3000$–4000. However, beyond $\sigma = 1.5$, the heat propagation described by $\rho_Q(m, t)$ becomes faster, necessitating a larger system size of $N = 8192$ but limiting us to a maximum time of only $t = 2000$. Despite this challenge, it should be emphasized that even reaching a time scale of $t = 2000$ is considered relatively long if compared with previous studies focused on SR systems with NN couplings [36–38], given that we are dealing with a LR interacting system.

From Fig. 3, it is evident that the central regions of $\rho_Q(m, t)$ at $\sigma = 2$ exhibit a flatter profile than the results obtained for other σ's. This observation further supports the distinctiveness of $\sigma = 2$. Additionally, apart from this noticeable difference, for all other considered σ's, $\rho_Q(m, t)$
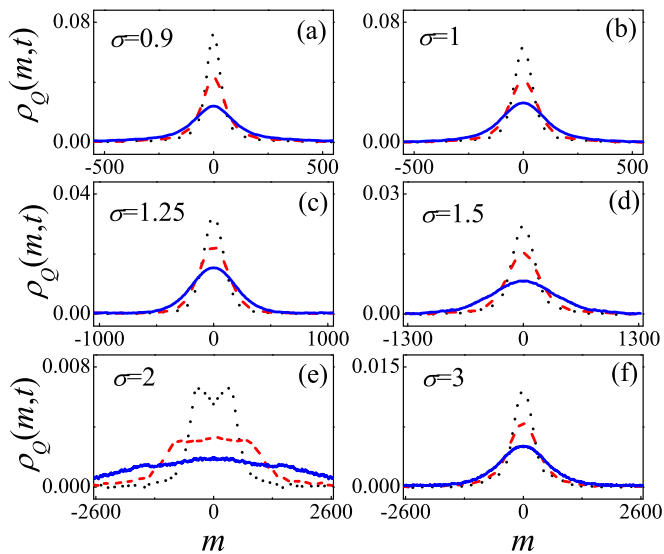
FIG. 3. $\rho_Q(m,t)$ for $0.9 \leqslant \sigma \leqslant 3$ for several typical long times, wherein the results of $0.9 \leqslant \sigma \leqslant 1.5$ are based on a system size of $N = 4096$ with a time up to $t = 3000$–4000 (note that, for $\sigma \leqslant 1.25$, the longest t is 4000, while in the case of $\sigma = 1.5$, the longest $t = 3000$); for $\sigma > 1.5$, we use a larger size of $N = 8192$ but with a time only up to $t = 2000$. Under these setups, in (a)–(c), the three long times are $t = 1000$ (dotted), $t = 2000$ (dashed), and $t = 4000$ (solid); in (d), they are $t = 1000$ (dotted), $t = 2000$ (dashed), and $t = 3000$ (solid); while in (e) and (f), they are $t = 500$ (dotted), $t = 1000$ (dashed), and $t = 2000$ (solid), respectively.

displays a single broadening central peak with time. This behavior is distinct from the three-peak profile (one central and two side peaks) observed in superdiffusive regimes of SR nonlinear momentum-conserving chains with NN couplings only, as demonstrated by the Lévy walk model of the single particle [39]. It also suggests that a real SR system has not yet been achieved even with $\sigma = 3$ at hand. Another interesting and significant finding is that some of the displayed behaviors in Figs. 3(a)–3(d), such as that shown in $\sigma = 1.25$, resemble Gaussian peaks typically observed in 1D momentum-nonconserving lattice systems [38]. This Gaussian-like peak provides additional evidence for thermal transport close to diffusive within the regime $1 \leqslant \sigma \leqslant 1.5$.

To further verify the presence of diffusive thermal transport, we proceed to analyze the heat diffusion property represented by $\rho_Q(m,t)$. To achieve this, it is important to note that, instead of studying the mean squared displacement of $\rho_Q(m,t)$ against t, due to significant fluctuations observed for large distances m, we focus on examining the space-time scaling behavior exhibited by the central peak $\rho_Q(0,t)$ decay of $\rho_Q(m,t)$. This approach has been previously employed in deducing long-term asymptotic heat spread behaviors in SR systems with NN couplings only [36–38] and LR-FPUT models [14,18,20], encompassing ballistic, superdiffusive, and diffusive transport phenomena, respectively. Specifically, if $\rho_Q(0,t) \sim t^{-1/\gamma}$ ($\frac{1}{2} \leqslant 1/\gamma \leqslant 1$) holds true based on the scaling formula derived from the Lévy walk model of the single particle [39], then we have

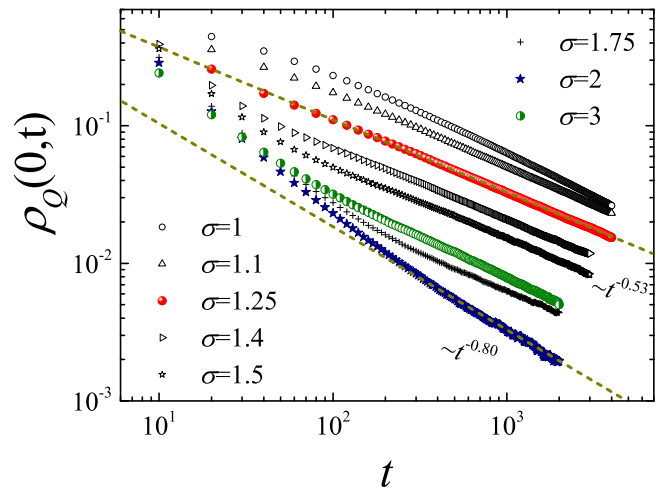$$t^{1/\gamma} \rho_Q(m,t) \simeq \rho_Q\left(\frac{m}{t^{1/\gamma}}, t\right). \tag{9}$$

FIG. 4. $\rho_Q(0,t)$ vs t in a log-log plot showing the detailed power-law decay in long times for $1 \leqslant \sigma \leqslant 3$. Here, note that, to highlight the central point of $\sigma = 1.25$, we start with $\sigma = 1$. In addition, the two dashed lines denote the best fittings of $\rho_Q(0,t) \sim t^{0.80}$ and $\rho_Q(0,t) \sim t^{0.53}$ for $\sigma = 2$ and 1.25, respectively.

Consequently, $1/\gamma = 1$, $\frac{1}{2} < 1/\gamma < 1$, and $1/\gamma = \frac{1}{2}$ correspond to ballistic, superdiffusive, and diffusive transport, respectively.

The log-log plot in Fig. 4 illustrates the variation of $\rho_Q(0,t)$ with respect to t for several representative values of σ ranging from 1 to 3. To emphasize the central point at $\sigma = 1.25$ within the range of $1 \leqslant \sigma \leqslant 1.5$, we start with the lowest σ value of $\sigma = 1$. It is evident that, among all considered values of σ, the decay is most rapid for $\sigma = 2$, characterized by an exponent $1/\gamma \simeq 0.80$. This finding, in light of the relationship derived from Lévy walks theory [39], i.e., $\alpha = 2 - \gamma$, suggests a value close to $\alpha \simeq 2 - 1.25 = 0.75$ (in our previous work [18], we yielded $1/\gamma \simeq 0.78$ and thus $\alpha \simeq 0.71$ for a short time). Interestingly, Ref. [40] has predicted a universality characterized by $\alpha = \frac{1}{4}$, while our results seem to imply another possible exponent of the universality described by $\alpha \simeq \frac{3}{4}$; even this is only numeric.

Beyond $\sigma = 2$, a series of exponents $1/\gamma$ have been observed in Fig. 4, based on the relatively long time considered. Some of these exponents, such as those for $\sigma = 1$ and 3, exhibit relatively larger values, while others are smaller. Before discussing the specific values, it is worth emphasizing the special case of $\sigma = 1.25$, where $1/\gamma \simeq 0.53$, which holds true for both short and long times. This scaling closely approximates diffusive behavior, considering the numerical error. Therefore, we speculate that, within the range $1 < \sigma \leqslant 1.5$, particularly around $\sigma = 1.25$, the thermal transport very close to diffusive seems to occur. This conjecture is reasonable since obtaining an exact result of $1/\gamma = \frac{1}{2}$ numerically is challenging, as $1/\gamma \simeq 0.53$ was also observed in a similar study on a 1D momentum-conserving lattice with a double-well potential [41,42], wherein the thermal transport very close to normal diffusive type has already been confirmed. Furthermore, additional intriguing information supporting diffusive thermal transport at $\sigma = 1.25$ seems evident from the data presented for $1 < \sigma \leqslant 1.5$: The result for $\sigma = 1.25$ just lies in the
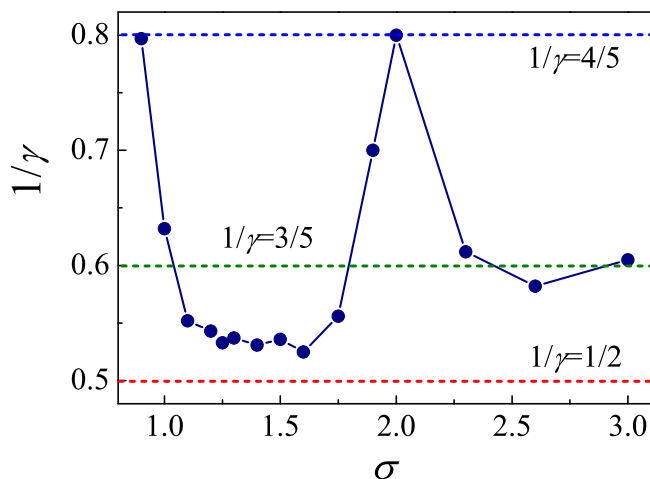
FIG. 5. $1/\gamma$ vs σ for $0.9 \leqslant \sigma \leqslant 3$, wherein the three dashed lines denote $1/\gamma = \frac{1}{2}, \frac{3}{5}$, and $\frac{4}{5}$, respectively.
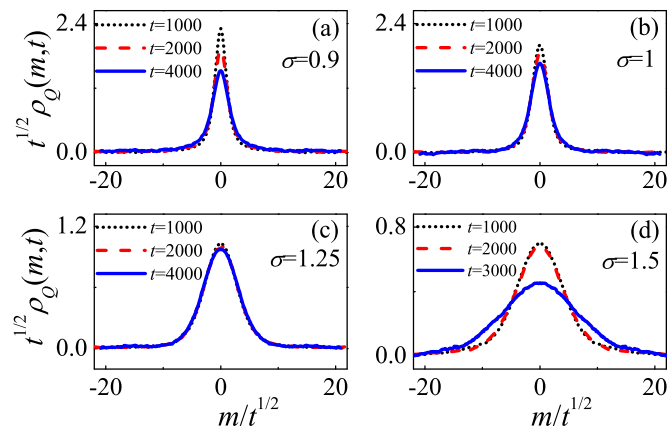

FIG. 6. The rescaled $\rho_Q(m, t)$ using the formula in Eq. (9) with $1/\gamma = \frac{1}{2}$ for (a) $\sigma = 0.9$, (b) $\sigma = 1$, (c) $\sigma = 1.25$, and (d) $\sigma = 1.5$.

whereas for $\sigma > 1.25$, the failure begins at a long time [see Fig. 6(d)].

middle between results obtained for other values of σ, indicating its central position within this range.

Now let us examine the detailed dependence of the scaling exponent $1/\gamma$ on σ within the range $0.9 \leqslant \sigma \leqslant 3$, as shown in Fig. 5. Some of the data are extracted from the best fittings presented in Fig. 4, while others are additionally calculated using the same methodology. We have to mention that all the data are based on the longest simulation times that we up to now can achieve. From Fig. 5, it is evident that, as σ increases from $\sigma = 0.9$ to $\sigma = 3$, $1/\gamma$ undergoes two rounds of decrease and one round of increase. In the first round ($0.9 \leqslant \sigma \leqslant 2$), with the increase of σ, $1/\gamma$ initially decreases from $\sim\frac{4}{5}$, reaching its minimum value $\sim\frac{1}{2}$. This minimum value persists for a wide range of σ around $\sigma = 1.25$, before increasing again up to $\sim\frac{4}{5}$ at $\sigma = 2$. During the second round ($2 \leqslant \sigma \leqslant 3$), $1/\gamma$ decreases from $\sim\frac{4}{5}$, converging toward a value $\sim\frac{3}{5}$. These results suggest a crossover from superdiffusive behavior ($\frac{1}{2} < 1/\gamma < 1$) to normal transport behavior ($1/\gamma = \frac{1}{2}$) for $0.9 \leqslant \sigma \leqslant 2$, likely occurring around $\sigma = 1.25$. This observation aligns with our previous conjecture based on Fig. 4. Furthermore, it indicates a crossover to a value of $\sim\frac{3}{5}$ for $\sigma > 2$. This, if combined with the Lévy walk theory [39], suggests $\alpha = 2 - \frac{5}{3} = \frac{1}{3}$, which closely matches the range $\alpha \in [0.3, 0.5]$ made for relevant SR systems with NN couplings only [17].

We are particularly interested in the subregime ($1 \leqslant \sigma \leqslant 1.5$) wherein the thermal transport close to diffusive can occur. Therefore, in Fig. 6, we further examine the result of rescaled $\rho_Q(m, t)$ under the diffusive scaling ($1/\gamma = \frac{1}{2}$) for several σ values around $\sigma = 1.25$. As can be seen, even though in both Figs. 4 and 5 the scaling exponents for $\sigma = 1, 1.25$, and 1.5, obtained by the best fittings are all close to $1/\gamma = \frac{1}{2}$, in Fig. 6, only the $\sigma = 1.25$ case gives the most approximate collapse for different times. This collapse further supports the observed transport close to diffusive around $\sigma = 1.25$ and provides strong evidence that $\sigma = 1.25$ appears to be the central point. It is also worth noting that, for $\sigma < 1.25$, the deviations of the collapse are more in short times [see Figs. 6(a) and 6(b)],

V. PHASE DIAGRAM OF THERMAL TRANSPORT

Considering the aforementioned understanding of the weak LR regime and in conjunction with the findings of Ref. [22] regarding the strong LR regime, we proceed to discuss the thermal transport phase diagram for this kind of LR-quartic FPUT-type system. Figure 7 presents a schematic representation of the inferred thermal transport phase diagram based on our current knowledge. On one hand, there are two notable points concerning σ: firstly, at $\sigma = 2$, the quasi-integrable or weakly nonintegrable dynamics occur [14,16,18]; secondly, at $\sigma = 0.5$, corresponding to the antipersistent energy current correlation, subdiffusive thermal transport is observed with a minimum negative value of $C_{JJ}(t)$ [22]. On the other hand, three distinct regimes, shaded, can be identified for transport of subdiffusive, diffusive, and SR-superdiffusive (we use this to distinguish it from the superdiffusive transport appearing in a real LR system), respectively. Within the considered long time range, subdiffusive transport is likely to occur for $0 \leqslant \sigma \leqslant 0.8$ since, beyond $\sigma \simeq 0.8$, the disappearance of antipersistent energy current correlation has been reported [22]. The observed thermal transport close to diffusive is expected around $\sigma = 1.25$, possibly within an interval $1 \leqslant \sigma \leqslant 1.5$ as inferred from Fig. 5. The onset of SR-superdiffusion corresponds to the SR cases and begins slightly above $\sigma = 2$. Apart from these three prominent regions, there exist additional regimes such as $0.8 < \sigma < 1$ and those around $\sigma = 2$
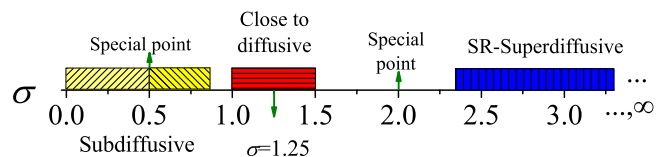

FIG. 7. The thermal transport phase diagram with respect to σ for the long-range (LR)-quartic Fermi-Pasta-Ulam-Tsingou (FPUT)-type system, wherein the three shaded sections, from left to right, correspond to the phases of subdiffusive, close to diffusive, and the short-range (SR)-superdiffusive, respectively.

represented by blanks that may potentially support superdiffusive transport but with different exponents of the universality; however, precise values of $1/\gamma$ in these regimes and their underlying mechanisms remain unclear and warrant further investigations.

VI. CONCLUSIONS

In summary, we have studied thermal transport in a 1D LR-quartic FPUT-type system, with our main focus on its weak LR regime ($1 \leqslant \sigma \leqslant 3$). In such a regime, authors of previous numerical studies on a similar model [14] and another LR-quadratic-quartic model [16], both with the Kac scaling factor $\frac{1}{N}$ included, have suggested superdiffusive thermal transport for all σ values, and the existing analytical results [19] can only provide partial predictions for $2 \leqslant \sigma \leqslant 3$. Remarkably and unexpectedly, our results here indicate that there is a subregime around $\sigma = 1.25$ wherein the thermal transport behaviors can be very close to the diffusive type. This finding is well supported, both by the fast exponential decay of the energy current correlations and by the space-time scaling close to Gaussian of the equilibrium heat correlations, with the long time range considered.

Combining our prior results on thermal transport in the strong LR regime in the same model [22], we have further provided a complete phase diagram for thermal transport in this LR-quartic model. This phase diagram indicates that, on one hand, for a large value $\sigma > 2$, even the thermal transport seems close to the predictions of the relevant SR systems, the exact exponent [$\alpha = \frac{2}{5}$ ($\gamma = \frac{8}{5}$) or $\alpha = \frac{1}{2}$ ($\gamma = \frac{3}{2}$)] in the SR limit (i.e., the systems with symmetric interparticle potentials) is still hard to reach, which then raises open problems in the future; on the other hand, for small σ within both the strong and weak LR regimes, the intermediate process of transport can be quite rich since both subdiffusive and normal diffusive thermal transports seem to occur. In addition, from this phase diagram, there are two previously found interesting special points of $\sigma = 2$ and 0.5, which give intriguing transport features, largely enriching the thermal transport in the system.

Turning to the recently identified normal thermal transport around $\sigma = 1.25$, its discovery is quite unexpected. It suggests that, by introducing appropriate LR interactions, even the momentum-conserving systems can still exhibit diffusive heat conduction satisfying Fourier's law. It thus implies that the possible physics of the underlying mechanism for Fourier's law in LR systems could be more complicated, if compared with the relevant SR systems with NN couplings only. In this respect, we would like to note that it has been recently revealed, with appropriate LR interactions, even a fully nonintegrable system with moving DBs as its primary microscopic excitations can still support ballistic thermal transport that previously occurred only in integrable systems [43]. Therefore, one would conjecture that possibly it is the emergence of moving DBs, together with various excitations and their scattering dynamics, leading to the observed thermal transport close to diffusive here. Viewing this, in Fig. 8, we present an additional evidence of phonon-DBs scattering dynamics for the three special points of $\sigma = 0.5$, 1.25, and 2, as indicated in
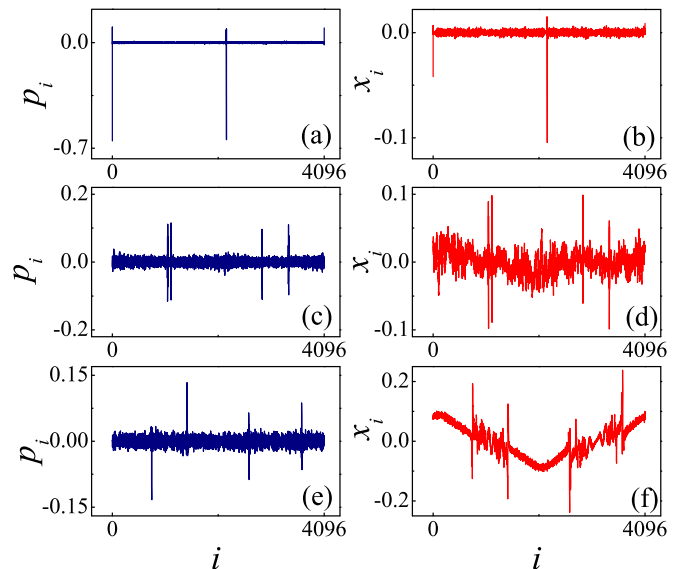

FIG. 8. Snapshots of momentum p_i and displacement x_i of the particle vs i at a given long time $t = 7000$, after initially applying two kicks at $i = 1$ and 2205 with momenta $p_1 = -0.7$ and $p_{2205} = 0.7$ (corresponding to an averaged temperature of $T = 0.5$), respectively, for the three special points (a) and (b) $\sigma = 0.5$, (c) and (d) $\sigma = 1.25$, and (e) and (f) $\sigma = 2$.

Fig. 7. This evidence is obtained by performing the following numerical experiment like those in Refs. [22,43], i.e., at time $t = 0$ when all particles are at their equilibrium positions (the system is not yet thermalized), we first apply two kicks at the locations of $i = 1$ and 2205 with momenta $p_1 = -0.7$ and $p_{2205} = 0.7$, respectively (it may correspond to an averaged temperature close to $T = 0.5$). We then carefully observe the evolution of the dynamics of the system. The snapshots of momentum p_i and displacement x_i of the particle versus i at a relatively long time $t = 7000$ are then depicted in Fig. 8. As can be seen, the case of $\sigma = 0.5$ indicates strong standing DBs [see Figs. 8(a) and 8(b)] with only few moving excitations presented, and so the subdiffusive transport has been observed, whereas both $\sigma = 1.25$ and 2 support moving DBs [see Figs. 8(c)–8(f)], which can interact with phonons, thus resulting in the transport either close to diffusive or superdiffusive. The strength of phonon-DB scattering of $\sigma = 1.25$ is obviously stronger than that in the case of $\sigma = 2$, which can be easily inferred by comparing the results of Figs. 8(d) and 8(f). This distinction is in accordance with the observed transport close to diffusive at $\sigma = 1.25$. We hope that this final evidence could provide some further insights, even though detailed studies of the phonon-DB scattering in this system are still required.

Overall, in this paper, we have systematically explored the thermal transport behavior in a LR-quartic model without including the Kac scaling factor $\frac{1}{N}$, within the weak LR regime. This result, together with our prior results within the strong LR regime [22] in the same model, then provides a comprehensive understanding of thermal transport in this kind of LR interacting FPUT-type model. It should be noted that,

as already mentioned in the Introduction, there are two other kinds of similar models of the LR-quadratic-quartic [16] and LR-quartic [14] systems both with $\frac{1}{N}$ presented, which seem to show distinct thermal transport behavior within both the strong and weak LR regimes. It thus raises questions on the roles of both the LR-quadratic term and the Kac scaling factor in thermal transport of 1D LR interacting FPUT-type models. We believe that these issues, inspired by this paper, are surely worth further exploration in upcoming research endeavors.

[1] T. Padmanabhan, Statistical mechanics of gravitating systems, Phys. Rep. **188**, 285 (1990).

[2] R. H. French, V. A. Parsegian, R. Podgornik, R. F. Rajter, A. Jagota, J. Luo, D. Asthagiri, M. K. Chaudhury, Y.-m. Chiang, S. Granick *et al.*, Long range interactions in nanoscale science, Rev. Mod. Phys. **82**, 1887 (2010).

[3] A. Campa, T. Dauxois, and S. Ruffo, Statistical mechanics and dynamics of solvable models with long-range interactions, Phys. Rep. **480**, 57 (2009).

[4] F. Bouchet, S. Gupta, and D. Mukamel, Thermodynamics and dynamics of systems with long-range interactions, Physica A **389**, 4389 (2010).

[5] Y. Levin, R. Pakter, F. B. Rizzato, T. N. Teles, and F. P. C. Benetti, Nonequilibrium statistical mechanics of systems with long-range interactions, Phys. Rep. **535**, 1 (2014).

[6] S. Gupta and S. Ruffo, The world of long-range interactions: A bird's eye view, Int. J. Mod. Phys. A **32**, 1741018 (2017).

[7] S. Lepri, *Thermal Transport in Low Dimensions: From Statistical Physics to Nanoscale Heat Transfer* (Springer, International Publishing, Cham, 2016).

[8] S. Lepri, R. Livi, and A. Politi, Thermal conduction in classical low-dimensional lattices, Phys. Rep. **377**, 1 (2003).

[9] A. Dhar, Heat transport in low-dimensional systems, Adv. Phys. **57**, 457 (2008)

[10] G. Benenti, D. Donadio, S. Lepri, and R. Livi, Non-Fourier heat transport in nanosystems, Riv. Nuovo Cim. **46**, 105 (2023).

[11] G. Benenti, S. Lepri, and R. Livi, Anomalous heat transport in classical many-body systems: Overview and perspectives, Front. Phys. **8**, 292 (2020).

[12] R. Livi, Heat transport in one dimension, J. Stat. Mech. (2020) 034001.

[13] C. Olivares and C. Anteneodo, Role of the range of the interactions in thermal conduction, Phys. Rev. E **94**, 042117 (2016).

[14] D. Bagchi, Thermal transport in the Fermi-Pasta-Ulam model with long-range interactions, Phys. Rev. E **95**, 032102 (2017).

[15] D. Bagchi, Energy transport in the presence of long-range interactions, Phys. Rev. E **96**, 042121 (2017).

[16] S. Iubini, P. Di Cintio, S. Lepri, R. Livi, and L. Casetti, Heat transport in oscillator chains with long-range interactions coupled to thermal reservoirs, Phys. Rev. E **97**, 032102 (2018).

[17] P. Di Cintio, S. Iubini, S. Lepri, and R. Livi, Equilibrium time-correlation functions of the long-range interacting Fermi-Pasta-Ulam model, J. Phys. A: Math. Theor. **52**, 274001 (2019).

[18] J. Wang, S. V. Dmitriev, and D. Xiong, Thermal transport in long-range interacting Fermi-Pasta-Ulam chains, Phys. Rev. Res. **2**, 013179 (2020).

[19] S. Tamaki and K. Saito, Energy current correlation in solvable long-range interacting systems, Phys. Rev. E **101**, 042118 (2020).

[20] D. Bagchi, Heat transport in long-ranged Fermi-Pasta-Ulam-Tsingou-type models, Phys. Rev. E **104**, 054108 (2021).

[21] D. Xiong and J. Wang, Subdiffusive energy transport and antipersistent correlations due to the scattering of phonons and discrete breathers, Phys. Rev. E **106**, L032201 (2022).

[22] D. Xiong and J. Wang, Antipersistent energy current correlations in strong long-ranged Fermi-Pasta-Ulam-Tsingou type models, Phys. Rev. E **109**, 044122 (2024).

[23] S. Iubini, S. Lepri, and S. Ruffo, Hydrodynamics and transport in the long-range-interacting φ^4 chain, J. Stat. Mech. (2022) 033209.

[24] L. Defaveri, C. Olivares, and C. Anteneodo, Heat flux in chains of nonlocally coupled harmonic oscillators: Mean-field limit, Phys. Rev. E **105**, 054149 (2022).

[25] F. Andreucci, S. Lepri, S. Ruffo, and A. Trombettoni, Classical and quantum harmonic mean-field models coupled intensively and extensively with external baths, SciPost Phys. Core **5**, 036 (2022).

[26] F. Andreucci, S. Lepri, S. Ruffo, and A. Trombettoni, Nonequilibrium steady states of long-range coupled harmonic chains, Phys. Rev. E **108**, 024115 (2023).

[27] C. Kittel, *Introduction to Solid State Physics* (Wiley, New York, 1996).

[28] J. Wang and A. C. Li, Dynamic crossover towards energy equipartition in the Fermi-Pasta-Ulam-Tsingou β model with long-range interactions, Phys. Rev. E **106**, 014135 (2022).

[29] H. Christodoulidi, T. Bountis, C. Tsallis, and L. Drossos, Dynamics and statistics of the Fermi-Pasta-Ulam β model with different ranges of particle interactions, J. Stat. Mech. (2016) 123206.

[30] F. Tamarit and C. Anteneodo, Rotators with long-range interactions: Connection with the mean-field approximation, Phys. Rev. Lett. **84**, 208 (2000).

[31] Y. Doi and K. Yoshimura, Symmetric potential lattice and smooth propagation of tail-free discrete breathers, Phys. Rev. Lett. **117**, 014101 (2016).

[32] S. Chen, Y. Zhang, J. Wang, and H. Zhao, Diffusion of heat, energy, momentum, and mass in one-dimensional systems, Phys. Rev. E **87**, 032153 (2013).

[33] M. P. Aüllen and D. L. Tildesley, *Computer Simulation of Liquids* (Clarendon, Oxford, 1987).

[34] S. Gupta, M. Potters, and S. Ruffo, One-dimensional lattice of oscillators coupled through power-law interactions: Continuum

limit and dynamics of spatial Fourier modes, Phys. Rev. E **85**, 066201 (2012).

[35] S. Chen, Y. Zhang, J. Wang, and H. Zhao, Finite-size effects on current correlation functions, Phys. Rev. E **89**, 022111 (2014).

[36] D. Xiong, Observing golden-mean universality class in the scaling of thermal transport, Phys. Rev. E **97**, 022116 (2018).

[37] D. Xiong, F. Thiel, and E. Barkai, Using Hilbert transform and classical chains to simulate quantum walks, Phys. Rev. E **96**, 022114 (2017).

[38] D. Xiong, D. Saadatmand, and S. V. Dmitriev, Crossover from ballistic to normal heat transport in the ϕ^4 lattice: If nonconservation of momentum is the reason, what is the mechanism? Phys. Rev. E **96**, 042109 (2017).

[39] V. Zaburdaev, S. Denisov, and J. Klafter, Lévy walks, Rev. Mod. Phys. **87**, 483 (2015).

[40] S. Tamaki, M. Sasada, and K. Saito, Heat transport via low-dimensional systems with broken time-reversal symmetry, Phys. Rev. Lett. **119**, 110602 (2017).

[41] D. Xiong, Crossover between different universality classes: Scaling for thermal transport in one dimension, Europhys. Lett. **113**, 14002 (2016).

[42] D. Xiong, Underlying mechanisms for normal heat transport in one-dimensional anharmonic oscillator systems with a double-well interparticle interaction, J. Stat. Mech. (2016) 043208.

[43] J. Wang and D. Xiong, Observation of ballistic thermal transport in a nonintegrable classical many-body system, arXiv:2402.02142.